UDK 543.428.3:620.1/.2
Original scientific article/Izvirni znanstveni članek

ISSN 1580-2949
MTAEC9, 44(2)73(2010)

AES AND XPS CHARACTERIZATION OF TITANIUM HYDRIDE POWDER

PREISKAVE PRAŠKA TITANOVEGA HIDRIDA S SPEKTROSKOPIJO AUGERJEVIH ELEKTRONOV IN RENTGENSKO FOTOELEKTRONSKO SPEKTROSKOPIJO

Irena Paulin, Djordje Mandrino, Črtomir Donik, Monika Jenko

Institute of Metals and Technology, Lepi pot 11, 1000 Ljubljana, Slovenia
irena.paulin@imt.si

Prejem rokopisa – received: 2009-12-01; sprejem za objavo – accepted for publication: 2009-12-24

Titanium hydride powder, manufactured by ball milling titanium in a hydrogen atmosphere down to micron-sized particles, was analyzed by X-ray Photoelectron Spectroscopy (XPS). A strong titanium oxide signal was also measured, which decreased somewhat after intense sputtering of the sample, but was impossible to get rid of completely. This was probably due to the high surface/volume ratio of each TiH_x particle, which contributes to a substantial titanium oxide/TiH_x ratio, and due to the surface morphology of the powder sample, which leaves a considerable part of the oxide layer shaded during the sputtering. Auger Electron Spectroscopy (AES) was then employed and some characteristic differences in the shape of the Ti LMM spectra between the TiH_x and Ti were observed; however, they can be ascribed to the TiH_x only after a comparison with the same types of spectra measured on titanium oxide. An additional XPS measurement was performed with TiH_x powder and powdered Ti. The peaks were fitted with Ti oxide and metallic Ti components and the shifts of the metallic component between the Ti and TiH_x (a shift of 0.4 eV was expected) were checked for.

Keywords: titanium hydride, ball milling, AES, XPS

Prašek titanovega hidrida, sintetiziran z mletjem titana v kroglič nem mlinčku v vodikovi atmosferi do mikrometrske velikosti delcev, smo analizirali z rentgensko fotoelektronsko spektroskopijo (XPS). Pri tem smo izmerili močan signal titanovega oksida, ki je sicer upadel po intenzivnem ionskem jedkanju površine vzorca, ni pa izginil. Verjeten razlog je visoko razmerje površina/volumen posameznih delcev TiH_x, ki prispeva k znatnemu razmerju titanov oksid/TiH_x, kakor tudi morfologija površine praškastega vzorca, zaradi katere je del oksida zasenčen med ionskim jedkanjem. S spektroskopijo Augerjevih elektronov (AES) smo opazili nekatere karakteristične razlike v obliki Ti LMM-spektrov med TiH_x in Ti, vendar jih je bilo mogoče pripisati TiH_x šele po primerjavi z enakim tipom spektrov, izmerjenih pri titanovem oksidu. Nadaljnjo meritev XPS smo opravili pri prašku TiH_x in prašku Ti. Določili smo oksidne in kovinske komponente vrhov in preverjali premike kovinskih komponent pri TiH_x glede na Ti (premik naj bi bil 0,4 eV).

Ključne besede: titanov hidrid, kroglični mlinček, AES, XPS

1 INTRODUCTION

Titanium hydride can be used as a catalyst in the reversible dehydrogenation of other hydrides and carbon nanotubes.[1,2,3] It is also used as a catalyst in the preparation of titanium compounds,[1,4,5] as a source of pure hydrogen,[1] in the manufacturing of ceramic and glass seals from a mixture of active metal titanium or titanium hydride in powder form [1,6] and titanium coatings.[1] It is also well known as a blowing agent in the production of aluminum foams and some other foam-like structures produced by powder metallurgy.[7,8] For these purposes extensive studies of titanium hydride as well as of dehydrogenation and their effect on the formation of alloy foams have been performed.[9,10] In this study an attempt was made to apply surface-analysis techniques (AES and XPS) to titanium hydride powder, manufactured by ball milling titanium in a hydrogen atmosphere, that is used for the commercial production of aluminum foam. It was shown previously that the characteristic signatures from ultra-high-vacuum (UHV) deposited thin-film titanium hydride can be obtained using these techniques.[11,12] In our case the titanium hydride was in the shape of micron-sized powder particles. Therefore, in the XPS a strong titanium oxide signal was also measured, which decreased somewhat after the intense sputtering of the sample, but was impossible to remove completely due to the high surface/volume ratio of each TiH_x particle, which contributes to the substantial titanium oxide/TiH_x ratio, and due to the surface morphology of the powder sample, which leaves a considerable part of the oxide layer shaded during the sputtering. This oxide component also influences the shape of the Ti LMM peaks. Thus, while relying on the same type of titanium hydride, the characteristic features in AES and XPS spectra, as observed by Lisowski et al.,[11] had to be resolved from rather complex data (due to the complexity of the system in this study compared to the system as described by Lisowski et al. [11]).

2 EXPERIMENTAL

Titanium hydride powder, milled titanium, polished titanium plate and titanium oxide powder samples were fixed onto sample holders for the SEM/AES/XPS inve-

stigations by means of UHV-compatible double-sided sticky tape. Th esputter cleaning of the samples was performed under UHV conditions inside the main vacuum chamber of the SEM/AES/XPS apparatus, where the samples were introduced via a fast-entry air-lock.

The SEM imaging as well as the AES and XPS depth profiling of the samples were performed using a VG-Scientific Microlab 310F SEM/AES/XPS. For all the XPS measurements, Mg K_α radiation at 1253.6 eV with an anode voltage × emission current = 12.5 kV × 16 mA = 200 W was used. For the XPS profiling measurements an Ar^+ energy of 3 keV at 1 μA ion current over a 6 × 6 mm^2 area was used. Similar ion-beam parameters with a 4 × 4 mm^2 area were used for the AES profiling. A rough estimate for the sputtering rate during the XPS profiling parameters is of the order of 1 nm/min, and 2 nm/min for the AES.

The AES and XPS spectra were acquired using the Avantage 3.41v data-acquisition & data-processing software supplied by the SEM/AES/XPS equipment manufacturer. Casa XPS software [13] was also used for detailed data processing.

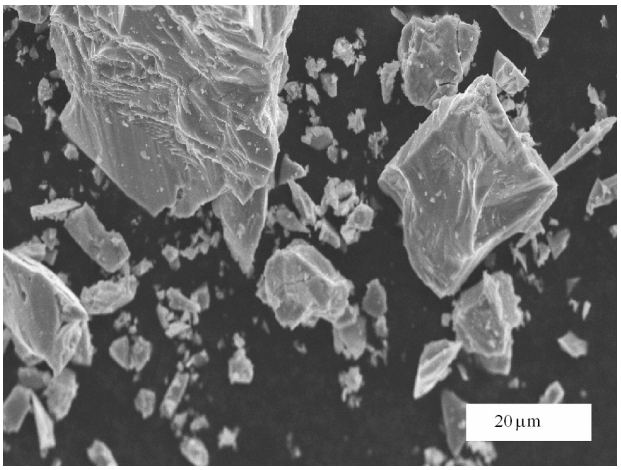

Figure 1: SEM image of the Ti hydride powder
Slika 1: SEM slika praška Ti hidrida

3 RESULTS AND DISCUSSION

A SEM image of the particles of as-received Ti hydride powder manufactured by the ball milling of titanium in a hydrogen atmosphere is shown in **Figure 1**. It can be seen that powder grains are of irregular shape, ranging over more than two orders of magnitude in size: from below 0.5 μm to well over 50 μm.

In **Figure 2,** high-resolution XPS spectra of the Ti 2p from pure Ti (**Figure 2a, line 1**) and Ti hydride (**Figure 2a, line2**), as measured by Lisowski et al. [11] on UHV-deposited thin films, are shown. The Ti 2p of Ti hydride at 1200 s (top), 8400 s and 36000 s sputtering times are shown in **Figure 2b**. The Ti 2p of the milled Ti at 1200 s (top), 4800 s and 8400 s sputtering times are shown in **Figure 2c**. While in the spectra of Lisowski et al. [11] the metallic-type Ti seems to be predominant, with an approximately 0.4 eV shift towards higher binding energies for Ti $2p_{3/2}$, in the case of the Ti hydride, the spectra measured on the ball-milled Ti and the Ti hydride are much more complex. Ti 2p peaks obtained were fitted with the Ti $2p_{3/2}$ and Ti $2p_{1/2}$ components of metallic Ti, TiO_2 and TiO_x.[14,15] The metallic Ti $2p_{3/2}$ is the right-most component. The Ti hydride powder appears to be covered by a TiO_2 layer, which is partially removed or/and reduced only after prolonged sputtering (**Figure**

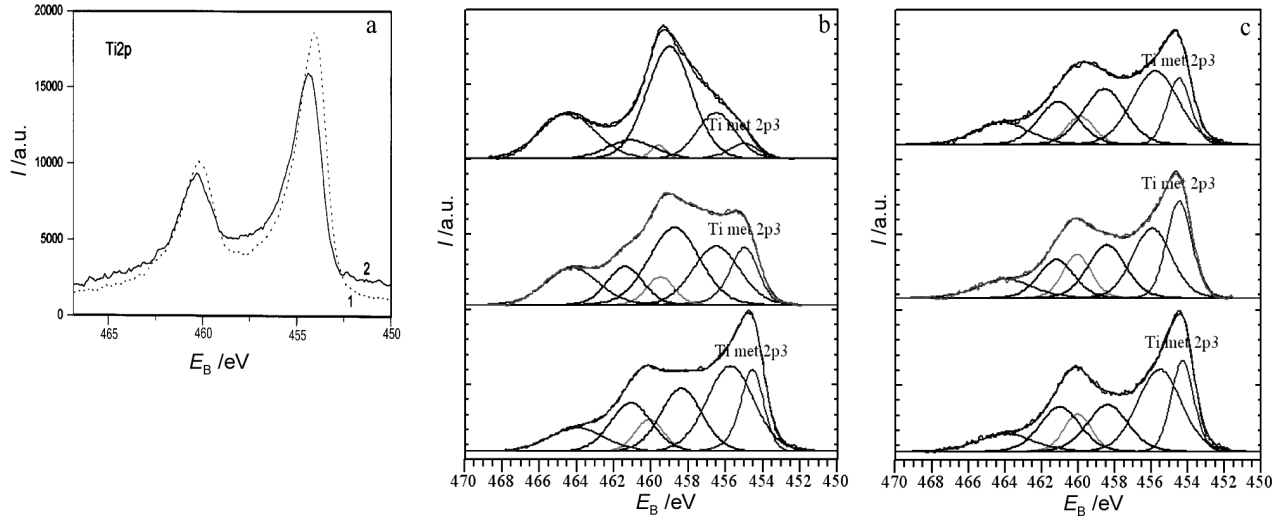

Figure 2: High-resolution XPS spectra of Ti 2p from pure Ti (dotted line 1) and Ti hydride (line 2) as measured by Lisowski et al. [11] on UHV-deposited thin films; Ti 2p of Ti hydride at 1200 s (top), 8400 s and 36000 s sputtering times (b); Ti 2p of milled Ti at 1200 s (top), 4800 s and 8400 s sputtering times (c).
Slika 2: Visokoločljivi spektri XPS-prehodov Ti 2p s čistega Ti (črtkana črta 1) in Ti- hidrida (črta 2), kot so jih izmerili Lisowski in sodelavci [11] na tankih plasteh, nanesenih v UHV; Ti 2p s Ti-hidrida po 1200 s (zgoraj), 8400 s in 36 000 s ionskega jedkanja (b); Ti 2p z mletega Ti po 1200 s (zgoraj), 4800 s in 8400 s ionskega jedkanja (c).

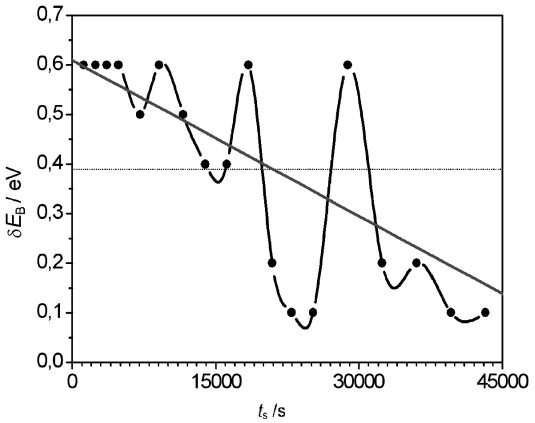

Figure 3: Deviation of the metallic Ti $2p_{3/2}$ binding energy with sputtering time for Ti hydride from the average value of 454.4 eV obtained for the milled Ti. The linear deviation trend (the thick solid line) and the average deviation (the thin horizontal line), which is close to 0.4 eV, are also shown.

Slika 3: Odvisnost razlike med vezavno energijo za kovinski Ti $2p_{3/2}$ Ti-hidrida in povprečno vrednostjo 454,4 eV, izmerjeno pri mletem Ti, od jedkalnega časa. Prikazana sta tudi linearen trend razlike (debela neprekinjena črta) in povprečna vrednost razlike (tanka vodoravna črta), ki je blizu 0,4 eV.

2b). The changes to the milled Ti with sputtering are much less pronounced, with TiO_x [16] and metallic Ti gaining slightly versus TiO_2 (**Figure 2c**). The average binding-energy value for the metallic Ti $2p_{3/2}$ component for the milled Ti can be determined from the XPS measurements after all sputtering cycles as (454.4 ± 0.1) eV.

In **Figure 3** the deviations, δE_B, of the metallic Ti $2p_{3/2}$ binding energy with sputtering time for Ti hydride from the average value of 454.4 eV determined for the milled Ti are shown. Also shown are the linear deviation trend and the average deviation, which is close to 0.4 eV. This can be interpreted as the Ti hydride characteristic shift in the metallic Ti $2p_{3/2}$ binding energy observed in Ti hydride thin films.[11] The highly scattered data are probably an artifact of the measurement as well as the fitting procedure. It is, nevertheless, possible to observe a declining deviation trend or even hypothesize about a possible switch from a high valued deviation (0.5–0.6 eV) to a low valued one (0.1–0.2 eV) in the 20 000–30 000 s sputtering time range. Whatever the precise form of this decline, it suggests that the Ti hydride powder

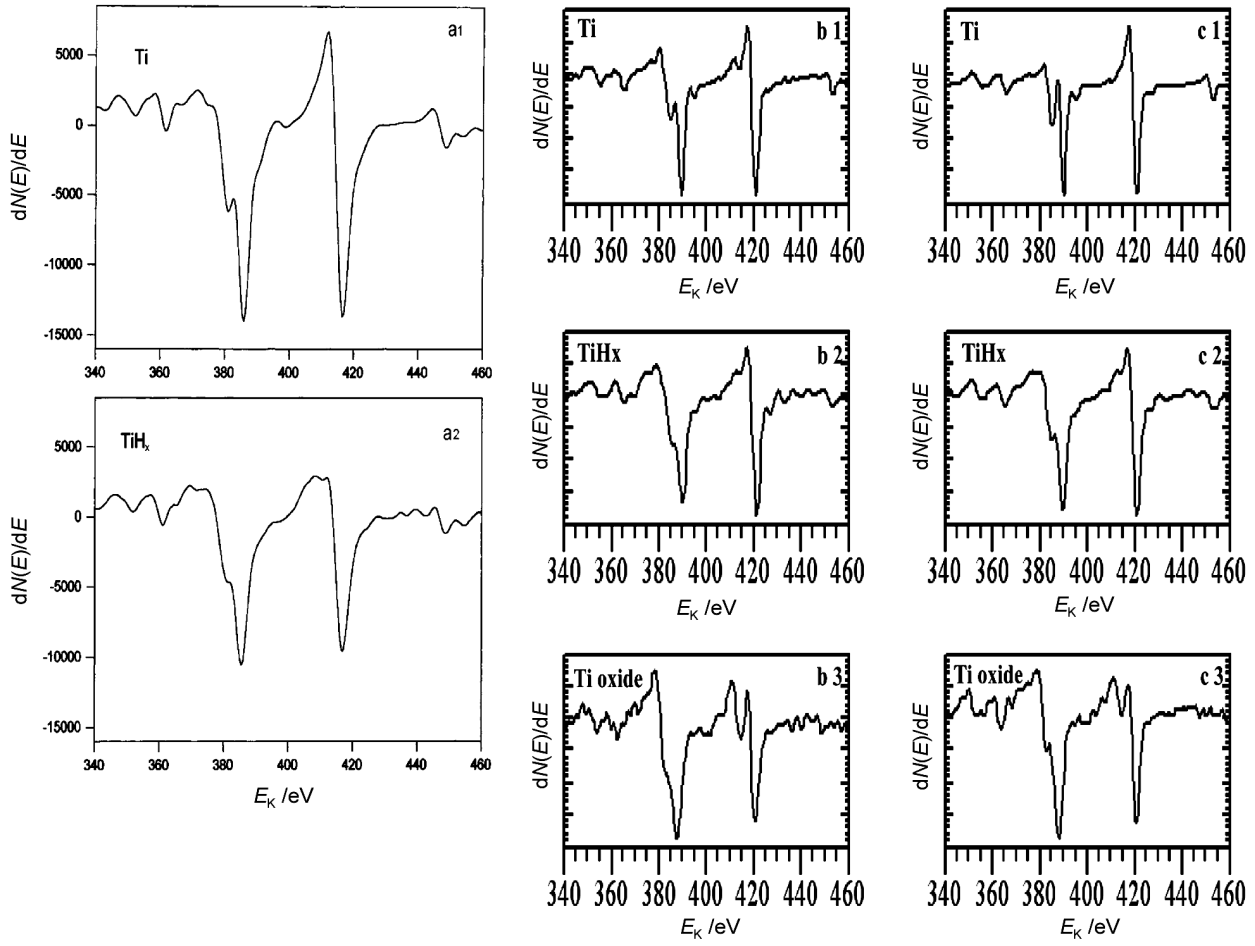

Fig 4: Ti LMM Auger transitions from pure Ti (a1) and Ti hydride (a2) as measured by Lisowski et al. [11] on UHV-deposited thin films; Ti LMM Auger transitions from pure Ti (b1, c1), Ti hydride (b2, c2) and Ti oxide (b3, c3) after 1200 s (b1, b2, b3) and 8400 s (c1, c2, c3) of sputtering.

Slika 4: Augerjevi prehodi Ti LMM s čistega Ti (a1) in Ti-hidrida (a2), kot so jih izmerili Lisowski in sodelavci[11] na tankih plasteh, nanesenih v UHV; Augerjevi prehodi Ti LMM s čistega Ti (b1, c1), Ti-hidrida (b2, c2) in Ti-oksida (b3, c3) po 1200 s (b1, b2, b3) in 8400 s (c1, c2, c3) ionskega jedkanja.

grains may not be of homogeneous consistency, with (more) hydrogen being closer to the grain surface.

In **Figure 4a** are the Ti LMM Auger transitions from pure Ti (**Figure 4a1**) and Ti hydride (**Figure 4a2**) as measured by Lisowski et al. [11] on UHV-deposited thin films. The Ti LMM Auger transitions from the polished Ti plate (**Figure 4b1**, **4c1**), the Ti hydride powder (**Figure 4b2**, **4c2**) and the TiO_2 powder (**Figure 4b3**, **4c3**) after 1200 s (**Figure 4b1**, **4b2**, **4b3**) and 8400 s (**Figure 4c1**, **Figure 4c2**, **Figure 4c3**) of sputtering are also shown. The differences in the peak shapes between all three samples can be observed and they become more pronounced with sputtering. The differences between the Ti hydride and the Ti do not completely agree with the differences found by Lisovski et al. [11]; however, it can be seen from **Figure 4** that they are not of the same nature as the differences between the Ti oxide and the Ti.

The most useful features are the less pointed shape of the maximum at approximately 375 eV [11], nearly dissappeared forking of TiH minimum between 385–390 eV and the small hydrogen-induced peak around 443 eV [11] in the spectra measured on the Ti hydride. Some other features also characteristic of Ti hydride may appear in these samples due to the Ti oxide.

4 CONCLUSIONS

XPS and AES characterizations of ball-milled Ti hydride powder were attempted using the same characteristic signatures in both methods as for Ti hydride thin films manufactured in UHV. Due to the manufacturing process the Ti hydride in this study was found to be covered with a layer of oxide that could not be completely removed, so the characteristic signal of Ti hydride could barely be extracted by peak fitting in the case of the XPS and had to be verified by comparison with metallic Ti and Ti oxide spectra in the case of AES. An additional benefit from the fitting of the Ti 2p is the suggestion that the titanium hydride grain may not have a homogeneous composition. To verify this, a cross-sectional AES study of individual grains by immersing titanium hydride powder in a low-melting-point alloy, and polishing the cross-section, a technique already used for study of soft-magnetic powders [17], is planned.

5 REFERENCES

[1] R. S. Venilla, A. Durygin, M. Merlini, Z. Wang, International Journal of Hydrogen Energy, 33 (**2008**), 6667–6671

[2] R. S Kumar, A. L. Cornelius, M. G. Pravica, M. F. Nicol, M. Y. Hu, P. C. Chow, Diam. & Relat. & Mater., 16 (2**007**), 1136–1139

[3] I. O. Bashkin, A. I. Koleshnikov, M. A. Adams, M. F. Nicol, M. Y. Hu, P.C. Chow, J. Phys. Condens. Matter., 12 (**2000**) 4757–4765

[4] M. N. Ozyagcilar, M.W. Davis; Catalysts for synthesis of ammonia, United States Patent 4623532, 1986

[5] V. E. Antonov, I. O. Bashkin, V. K. Fedotov, S. S. Khasanov, T. Hansen, A. S. Ivanov, Phys Rev B, 73 (**2006**)5, 054107–054112

[6] I. Paulin, C. Donik, M. Jenko, Mechanisms of HF Bonding in Dry Scrubber in Aluminium Electrolysis, Materiali in Tehnologije, 43 (**2009**) 4, 189

[7] PM Proa-Flores, RAL Drew, Advanced Engineering Materials, 10 (**2008**)9, 830–834

[8] A. Ibrahim, C. Koerner, R. F. Singer, Advanced Engineering Materials, 10 (**2008**), 845–848

[9] Y. W. Gu, M. S. Yong, B. Y. Tay, C. S. Lim, Materials Science & Engineering C, 29 (**2009**), 1515–1520

[10] M. Vijay, V. Selvarajan, K. P. Sreekumar, J. Yu, S. Liu, P.V. Ananthapadmanabhan, Solar Energy Materials & Solar Cells, 93 (**2009**), 1540–1549

[11] W. Lisowski, A. H. J. van den Berg, D. Leonard, H. J. Mathieu, Surface and Interface Analysis, 29 (**2000**), 292–297

[12] A. Kocijan, C. Donik, M. Jenko, The Corrosion Behaviour of duplex stainless steel in chloride solutions studied by XPS, Materiali in Tehnologije, 43 (**2009**) 4, 195

[13] Fairley N, CasaXPS VAMAS Processing Software. Available from World Wide Web: http://www.casaxps.com/

[14] Chastain J. (ed.), Handbook of X-ray Photoelectron Spectroscopy, Physical Electronics, Eden Prairie 1995

[15] C. D. Wagner, A.V. Naumkin, A. Kraut-Vass, J. W. Allison, C. J. Powell, J. R. Rumble (eds.), NIST X-ray Photoelectron Spectroscopy Database. Available from World Wide Web: http://srdata.nist.gov/xps

[16] C. Donik, A. Kocijan, I. Paulin, M. Jenko, The Oxidation of Duplex Stainless Steel at Moderately Elevated Temperatures, Materiali in Tehnologije, 43 (**2009**) 3, 137

[17] M. Godec, Dj. Mandrino, B. Šuštaršič, M. Jenko, Surface and Interface Analysis, 34 (**2002**), 346–351